Journal of Colloid and Interface Science 360 (2011) 760–767

Contents lists available at ScienceDirect

Journal of Colloid and Interface Science

www.elsevier.com/locate/jcis

Kinetics and thermodynamic study of aniline adsorption by multi-walled carbon nanotubes from aqueous solution

Hind Al-Johani [a,b], Mohamed Abdel Salam [a,*]

[a] Chemistry Department, Faculty of Science, King Abdulaziz University, P.O. Box 80203, Jeddah 21589, Saudi Arabia
[b] Center of Excellence in Environmental Studies, King Abdulaziz University, P.O. Box 80216, Jeddah 21589, Saudi Arabia

ARTICLE INFO

Article history:
Received 12 March 2011
Accepted 26 April 2011
Available online 4 May 2011

Keywords:
Carbon nanotubes
Aniline
Adsorption
Kinetics
Thermodynamics

ABSTRACT

Multi-walled carbon nanotubes (MWCNTs) were used in the adsorptive removal of aniline, an organic pollutant, from an aqueous solution. It was found that carbon nanotubes with a higher specific surface area adsorbed and removed more aniline from an aqueous solution. The adsorption was dependent on factors, such as MWCNTs dosage, contact time, aniline concentration, solution pH and temperature. The adsorption study was analyzed kinetically, and the results revealed that the adsorption followed pseudo-second order kinetics with good correlation coefficients. In addition, it was found that the adsorption of aniline occurred in two consecutive steps, including the slow intra-particle diffusion of aniline molecules through the nanotubes. Various thermodynamic parameters, including the Gibbs free energy change (ΔG°), enthalpy change (ΔH°) and entropy change (ΔS°), were calculated. The results indicated that the spontaneity of the adsorption, exothermic nature of the adsorption and the decrease in the randomness reported as ΔG°, ΔH° and ΔS°, respectively, were all negative.

1. Introduction

A common problem in most industries is the disposal of large volumes of wastewater containing potentially toxic organic solutes. Considering general safety and the environmental consequences of these solutes, their presence in wastewater requires treatment prior to disposal. Aniline is one of the most common pollutants found in effluents from the pharmaceutical, pesticide, dyestuff, petrochemicals and agrochemical industries. Aniline harmfully affects both public health and environmental quality. Aniline-containing wastewater has created a series of serious environmental problems due to its high toxicity and environmental accumulation. Strict limits on the release of aniline have been established. Traditionally, aniline-containing wastewater is treated with photodecomposition [1–3], electrolysis [4], adsorption [5,6], oxidation [7,8], biodegradation [9] and other processes. Generally, adsorption technology has proved to be one of the most effective techniques in the separation and removal of a wide variety of organic pollutants from wastewater [10,11]. These techniques do not produce harmful byproducts, and the regeneration of both the adsorbent and pollutants is possible. One challenge faced by adsorption technologies is the discovery of new adsorbents that successfully remove organic pollutants, such as aniline, from aqueous solutions.

Carbon nanotubes (CNTs) are a relatively new adsorbent that have been shown to possess great potential for removing many types of pollutants. Examples of the potential of CNTs for the removal of several types of pollutants include the following: ionizable organic compounds from water [12,13]; dichlorodiphenyltrichloroethane and its metabolites at trace levels from water samples [14]; organophosphorus pesticides from wastewater sludge [15]; nicosulfuron, thifensulfuron-methyl and metsulfuron-methyl from water samples [16]; atrazine from aqueous solutions [17–19]; polyhalogenated organic pollutants from environmental water samples [20–24]; tetrabromobisphenol A [25], pharmaceuticals from spiked water samples [26]; drugs from urine samples [27]; viruses from water [28]; polyaromatic hydrocarbons [29]; thiamethoxam, imidacloprid and acetamiprid [30]; polycyclic aromatic hydrocarbons from environmental water [31]; and pesticides [32] and metal ions [33–38] from various environments. The remediation ability of CNTs relative to other adsorbents is due to its strong interactions with the pollutants. This interaction results from the delocalized electrons in hexagonal arrays of carbon atoms on the surface of CNTs.

Although it has been reported that carbon nanotubes have strong adsorption capabilities for various pollutants, the literature detailing the removal of organic compounds, such as aniline, using CNTs is still scarce [11,39,40]. Further investigations on the adsorption/removal of aniline using carbon nanotubes in an aqueous environment are needed. In this study, various carbon nanotubes were used to study the removal/adsorption of aniline from an aqueous solution. The effects of various operating parameters, such

* Corresponding author. Fax: +966 2 6952292.
E-mail address: masalam16@hotmail.com (M.A. Salam).

0021-9797/$ - see front matter © 2011 Elsevier Inc. All rights reserved.
doi:10.1016/j.jcis.2011.04.097

as solution pH, temperature, and aniline concentration, were studied and optimized. In addition, the type and mass of the carbon nanotubes was considered. The kinetics and thermodynamics of the adsorption process of aniline were studied. Kinetic studies are important to understand the factors and transport mechanisms that affect aniline interactions with an adsorbent, such as multi-walled carbon nanotubes (MWCNTs), and to determine the conditions that affect these interactions. Thermodynamic calculations of the adsorption process are required to understand the mechanism of adsorption, spontaneity, and heat of adsorption using different thermodynamic parameters.

2. Materials and methods

2.1. Materials

Two different diameters of multi-carbon nanotubes (MWCNTs) were used in this study. Short multi-walled carbon nanotubes with average diameters of 10–20 nm [SMWCNTs (10–20)] and short multi-walled carbon nanotubes with average diameters of 40–60 nm [SMWCNTs (40–60)] were obtained from Shenzhen Nano-Technologies, China (MWCNTs Shenzhen) and were used as received. All chemicals used in this study were obtained from Sigma–Aldrich (analytical grade), and all solutions were prepared using deionized water.

2.2. Characterization techniques

A transmission electron microscope (TEM) (type JEOL JEM-1230 operating at 120 kV attached to a CCD camera) was used to characterize the MWCNTs morphological structure. The specific surface area of the MWCNTs was determined from nitrogen adsorption/desorption isotherm measurements at 77 K using a model NOVA 3200e automated gas sorption system (Quantachrome, USA).

2.3. Adsorption experiment

Adsorption experiments were performed to determine the effect of time and temperature on the adsorption process and to identify the adsorption rate. The experimental procedures were performed as follows: (1) a series of solutions of various aniline concentrations were prepared; (2) the initial pH was measured, and a defined amount of the MWCNTs was then added to the solution; (3) these solutions were agitated on a magnetic stirrer for a certain period of time at room temperature; (4) at defined time points, a certain volume of the solution was removed and immediately filtered to collect the supernatant; and (5) the residual aniline concentration in the supernatant was determined using a UV/Vis instrument. The amount of aniline adsorbed was determined by measuring the difference in concentration between samples that were obtained at two consecutive time intervals over the course of the adsorption experiment. The adsorption capacity of the MWCNTs, q_t (mol g^{-1}), which represents the amount of aniline adsorbed per amount of MWCNTs, was calculated using a mass–balance relationship:

$$q = \frac{(C_o - C_t)V}{m} \quad (1)$$

where C_o and C_t are the concentrations of aniline in solution (mol L^{-1}) at time $t = 0$ and t, respectively. V is the volume of the solution (L) and m is the mass of the dry adsorbent used (g). The kinetic curves obtained were analyzed using various-order kinetic equations to obtain the parameters for understanding the adsorption process.

3. Results and discussion

3.1. Characterization of multi-walled carbon nanotubes

Transmission electron microscope imaging was used to study the morphological structure of the pristine MWCNTs; representative images are presented in Fig. 1. The outer diameters and inner cavities of MWCNTs (10–20) were 20–30 nm and 5–8 nm, respectively. The outer diameters and inner cavities of SMWCNTs (40–60) were 30–70 nm and 8–12 nm, respectively. In addition, the TEM analysis verified the hollow structure of the MWCNTs. Nitrogen adsorption/desorption isotherms for the pristine SMWCNTs (10–20) and SMWCNTs (40–60) were determined from a N_2 adsorption isotherm measured at 77 K; the results are presented in Fig. 2. According to the original IUPAC classification, the isotherms obtained from the different samples could be classified as type IV isotherms with H3 type hysteresis loops. However, according to the extended classification of the adsorption isotherms, the obtained isotherms could be classified as type IIb isotherms. The BET specific surface areas for SMWCNTs (10–20) and SMWCNTs (40–60) were 116.1 $m^2 g^{-1}$ and 79.2 $m^2 g^{-1}$, respectively. This indicted a higher specific surface area for MWCNTs 10–20 relative to MWCNTs 40–60.

3.2. Method development for the determination of aniline

Fig. 3 shows the aniline calibration curve that was determined using a UV/Vis spectrophotometer. The analytical figures of merit to measure aniline concentration using a UV/Vis spectrophotome-

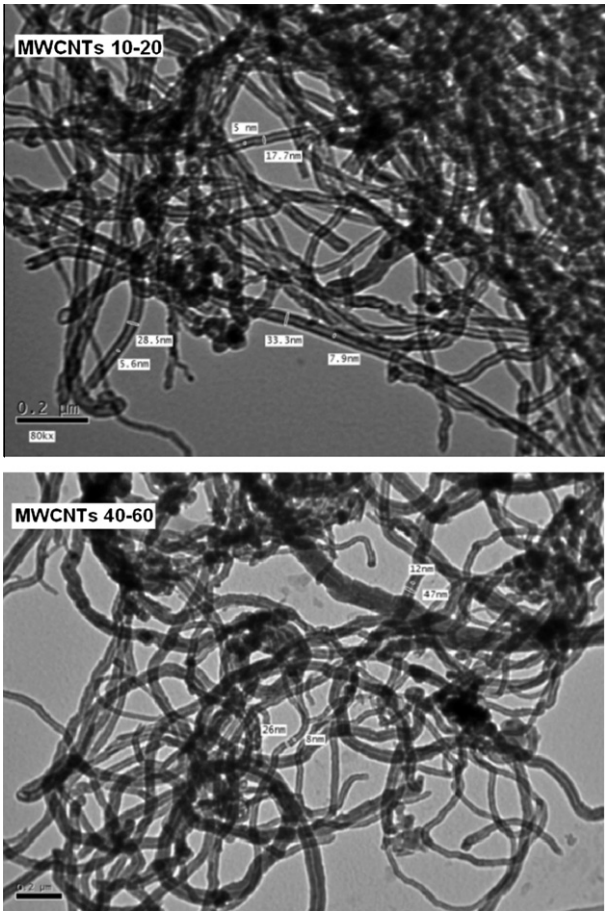

Fig. 1. Transmittance electron microscope images for the various MWCNTs.

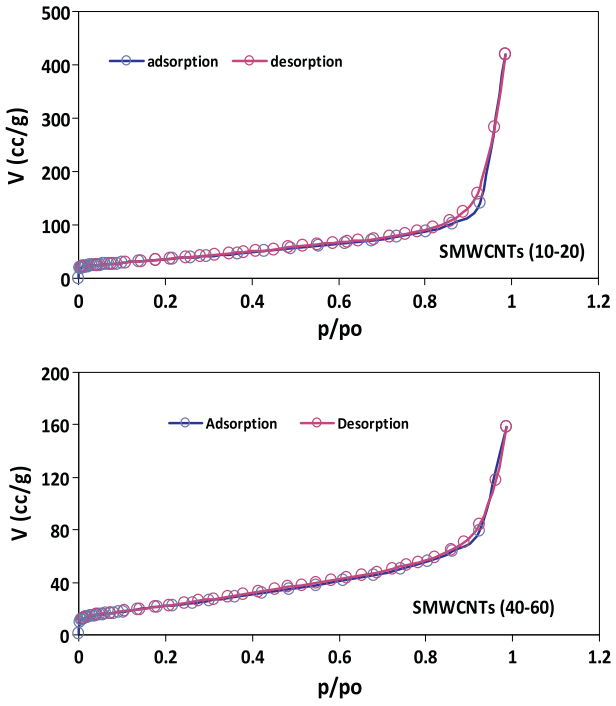

Fig. 2. Adsorption/desorption of nitrogen at 77 K.

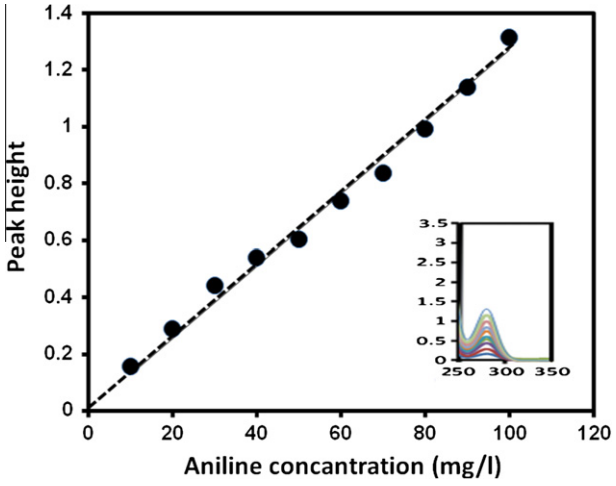

Fig. 3. The aniline calibration curve using a UV–Vis spectrophotometer. The insert shows the UV–Vis spectrum of the aniline samples.

ter were calculated from its calibration curve. These figures are presented in Table 1. The calibration curve was linear for aniline within the experimental concentration range, 10–100 mg/l (1×10^{-4}–1×10^{-3} M), with a correlation coefficient (R^2) value of 0.989. The sensitivity of the spectrophotometer for the determination of aniline in an aqueous solution was calculated from the slope of the calibration curve and was 0.0123. The limit of detection (LOD), defined as the concentration that produces a signal that is three times the standard deviation of the blanks (signal/noise ratio of 3), was measured by integrating blank peak areas of aniline from ten (10) independent samples using deionized water as the blank. The LOD was 2.76 mg/l. The limit of quantification (LOQ) is the lowest analyte concentration that can be quantified in a sample with acceptable relative standard deviation (RSD) under the stated operational conditions. The LOQ, 9.20 mg/l, was determined to be the analyte concentration corresponding to a signal/noise ratio of 10. The average relative standard deviation was 9.0% that confirms the good reproducibility of the UV/Vis spectrophotometer in the determination of the aniline.

Table 1
Figures of merit in the determination of aniline in an aqueous solution using a UV–Vis spectrophotometer.

Figures of merit	Value
Linear dynamic range (LDR)	10–100 mg/l
Sensitivity (slope of the calibration curve)	0.0123
Correlation coefficient (R^2)	0.989
Limit of detection (LOD) (mg/l)	2.76
LOQ: limit of quantification (mg/l)	9.20

3.3. Adsorption study

3.3.1. The effect of adsorption parameters

The effect of varying the parameters that affect the adsorption of aniline from an aqueous solution was investigated to optimize the adsorption process. The effect of carbon nanotubes dosage on the adsorption process was studied, and the results are illustrated in Fig. 4. It is clear from the figure that the percentage of aniline removed from the aqueous solution increased from 43% to 94% when the MWCNTs 10–20 dose increased from 10 mg to 40 mg. Increasing MWCNTs 40–60 dose from 10 mg to 40 mg also increased the percentage of aniline removed, from 20% to 92%. The increase in the percentage of aniline removed from the aqueous solution is primarily due to the greater number of active sites available for adsorption as a result of the increased amount of carbon nanotubes present. Especially at low doses, MWCNTs 10–20 had higher adsorption rates relative to MWCNTs 40–60. This observation may be due to the higher specific surface area of MWCNTs 10–20, 116.1 $m^2\ g^{-1}$, relative to MWCNTs 40–60, 79.2 $m^2\ g^{-1}$. A dose of 30 mg of carbon nanotubes was used for the further studies.

The effect of the solution pH on the removal of aniline by carbon nanotubes was also studied. Using diluted solutions of hydrochloric acid and sodium hydroxide, the pHs were adjusted, and the results are presented in Fig. 5. At an acidic pH of 3.0, which is lower than the p*K*a value of aniline (4.6), the percentage of aniline removed from aqueous solution was very low. This low adsorption is primarily due to the electrostatic repulsion between the positively charged protonated carbon nanotubes and the positively charged aniline molecules [41,42]. Increasing the pH from 3.0 to 5.0, which is higher than the p*K*a of aniline, enhanced the percentage of aniline removed to 80% and 68% for MWCNTs 10–20 and

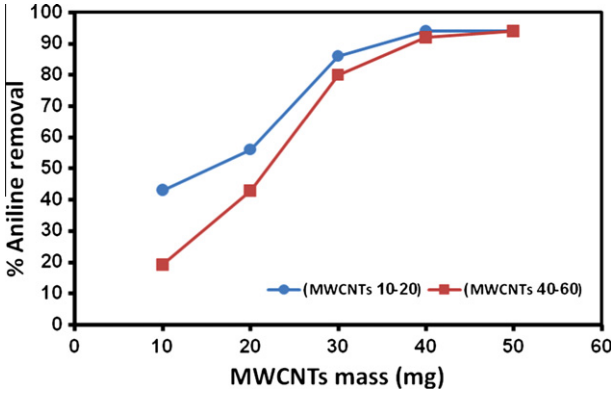

Fig. 4. Effect of MWCNTs mass on the adsorption of aniline from an aqueous solution. (experimental conditions: 20 ml solution, pH 7.0, 298 K, and aniline concentration 50 mg/l).

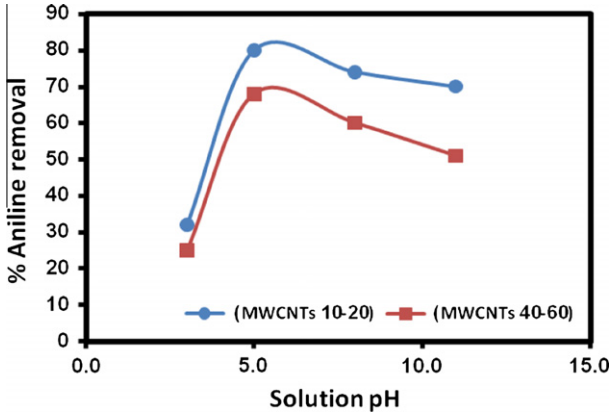

Fig. 5. Effect of the solution pH on the adsorption of aniline by different MWCNTs. (experimental conditions: 20 ml solution, 30 mg CNTs, 298 K, 30 min and, aniline concentration 50 mg/l).

MWCNTs 40–60, respectively. At a pH of 8.0, the percentage of aniline removed from the solution decreased slightly to 74% and 60% for MWCNTs 10–20 and MWCNTs 40–60, respectively. Under slightly basic conditions, aniline presents as negatively charged ions and carbon is negatively charged as well. Dispersive interactions are expected to predominate in this pH range. This was confirmed by increasing the solution pH to 11.0. At this pH, the percentage of aniline removed decreased to 70% and 51% for MWCNTs 10–20 and MWCNTs 40–60, respectively. A pH of 7.0 was selected for further studies.

The effect of aniline concentration on its removal by carbon nanotubes was studied, and the results are shown in Fig. 6. It is clear from the figure that increasing the aniline concentration while keeping the dose of carbon nanotubes constant led to a significant decrease in the percentage of aniline removed from an aqueous solution. Increasing the concentration from 10 mg/l to 100 mg/l decreased the percent of aniline removed from the solution from 64% to 36% and from 47% to 16% for the MWCNTs 10–20 and MWCNTs 40–60, respectively. These results are due to the limited number of active sites available for aniline adsorption.

The temperature of the solution was considered to be a critical factor affecting the adsorption process. If the removal efficiency of a certain pollutant from an aqueous solution is temperature dependent, which occurs in most cases, then it might affect the suitability of the adsorbent. The effect of solution temperature on aniline removal was studied at four different temperatures: 278 K, 298 K, 313 K and 333 K. The results are presented in Fig. 7. It is obvious from the figure that increasing the temperature

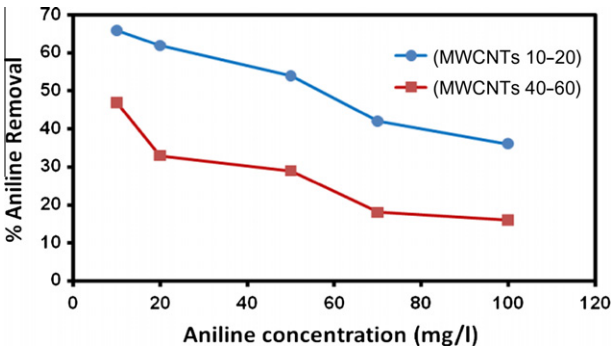

Fig. 6. Effect of aniline concentration on the adsorption of aniline from an aqueous solution by MWCNTs. (experimental conditions: 20 ml solution, pH 7.0, 298 K, 30 min and 30 mg CNTs).

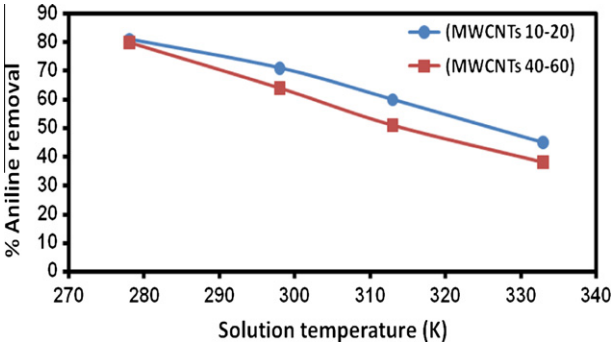

Fig. 7. Effect of the solution temperature on the adsorption of aniline from an aqueous solution by MWCNTs. (experimental conditions: 20 ml solution, pH 7.0, 30 mg CNTs, 30 min and aniline concentration 50 mg/l).

significantly affected the percentage of aniline removed from solution by carbon nanotubes. Increasing the temperature from 278 K to 333 K linearly decreased the percentage of aniline adsorbed and removed from the solution. At 278 K, 298 K, 313 K and 333 K, the percentage of aniline adsorbed decreased to 81%, 71%, 60% and 48% for MWCNTs 10–20, respectively; these percentages decreased to 80%, 64%, 51% and 38% for MWCNTs 40–60, respectively. This result suggests an exothermic nature of the adsorption process.

The effect of the contact time on the removal of aniline by carbon nanotubes was studied, and the results are shown in Fig. 8. It is obvious from the figure that increasing the contact time enhanced the adsorption process. This effect was especially observed within the first 30 min when most of the aniline was adsorbed. The percentage of aniline removal reached equilibrium within 3 h. It seems that the adsorption of aniline on carbon nanotubes occurred in two consecutive steps. The first step, which was the fastest, was the transfer of the aniline molecules from the aqueous phase to the external surface of carbon nanotubes. The second slower step was the diffusion of the aniline molecules between the carbon nanotubes bundles.

3.3.2. Kinetics and thermodynamic studies

Kinetics involves the study of the rates of chemical processes and facilitates an understanding of the factors that influence those rates. The study of chemical kinetics involves careful monitoring of the experimental conditions that influence the speed of a chemical reaction in its race toward equilibrium. These studies yield infor-

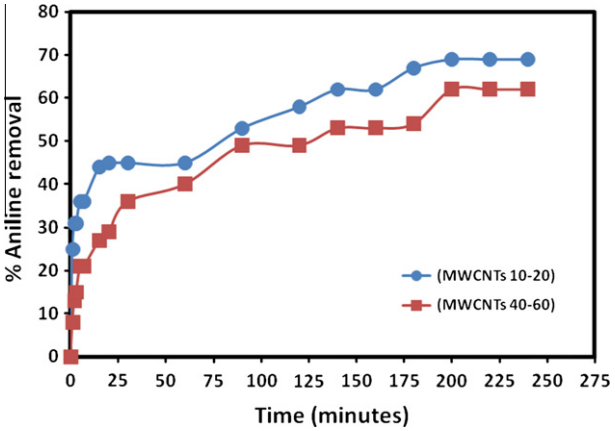

Fig. 8. Effect of the contact time on the adsorption of aniline from an aqueous solution by different MWCNTs. (experimental conditions: 20 ml solution, pH 7.0, 30 mg CNTs, 298 K and aniline concentration 50 mg/l).

mation about the possible mechanisms of adsorption and the different transition states formed on the way to a final adsorbate–adsorbent complex. The data obtained is used to develop appropriate mathematical models to describe the interactions. Once the reaction rates and the dependent factors are unambiguously known, these results can be utilized to develop adsorbent materials for industrial applications. The models are useful in understanding the complex dynamics of the adsorption process.

The effect of temperature on the removal of aniline from an aqueous solution by two different MWCNTs was studied kinetically, and the results are presented in Fig. 9. It is clear from the curves that the removal process was inhibited by increasing the solution temperature. This inhibition is indicative of the exothermic nature of the adsorption process, which will be discussed in detail below in the thermodynamic section. The curves of aniline adsorption exhibited two distinct phases. The first phase (initial steep slope) indicates the instantaneous adsorption of the aniline molecules over approximately 30 min. This steep slope may be attributed to the diffusion of the aniline molecules from the aqueous phase to the outer-surface of the solid MWCNTs. The initial adsorption reached equilibrium gradually, exhibiting a classic physisorption process. The second phase exhibits a gradual attainment of equilibrium due to the intra-particle diffusion of the aniline molecules between the MWCNTs. The kinetic adsorption data was processed to understand the dynamics of the adsorption process in terms of the order of the rate constant. Adsorption kinetics can be analyzed using several models. The pseudo-firstorder Lagergren equation and the pseudo-second order rate equation as shown below as Eqs. (2) and (3), respectively.

$$\ln(q_e - q_t) = \ln q_e - k_1 t \tag{2}$$

$$\frac{t}{q_t} = \frac{1}{k_2 q_e^2} - \frac{1}{q_e} t \tag{3}$$

In these equations, k_1 is the rate constant of the pseudo-first-order adsorption (min^{-1}), k_2 ($g\,mol^{-1}\,min$) is the rate constant of the pseudo second-order adsorption, q_e and q_t are the amounts of aniline adsorbed on adsorbent ($mol\,g^{-1}$) at equilibrium and at time t, respectively. The plotting of log (q_e–q_t) versus time (t) for the pseudo-first order kinetic model did not converge well and did not produce straight lines at the studied temperatures.

When the pseudo-second order adsorption equation was applied by plotting (t/q_t) versus time (t), all of the data converged well into a straight line with a high correlation coefficient (R^2). Based on these results, it is clear that the equilibrium adsorption from the pseudo-second order model is much closer to the experimental data as shown in Fig. 10. The pseudo-second order adsorption parameters, the rate constant (k_2), and the amount of aniline adsorbed (q_e) on MWCNTs at equilibrium were calculated from the slope and the intercept. The results are tabulated in Table 2. The values of k_2 increased with increasing solution temperature to 533.43, 729.24, 832.54, and 1732.2 for MWCNTs 10–20 at 298 K, 308 K, 313 K, and 323 K, respectively; these values were 276.08, 540.38, 600.42, and 845.36 for MWCNTs 40–60 at 298 K, 308 K, 313 K, and 323 K, respectively. Meanwhile, the values of q_e decreased with increasing the solution temperature to 2.49, 1.74, 1.24, and 0.799 for MWCNTs 10–20 at 298 K, 308 K, 313 K, and 323 K, respectively; these values were 2.24, 1.71, 1.38, and 0.907 for MWCNTs 40–60 at 298 K, 308 K, 313 K, and 323 K, respectively. The calculated q_e values are consistent with the experimental data. The relationship between the calculated amount of aniline adsorbed (q_e) on the MWCNTs at equilibrium was plotted against the solution temperature for both MWCNTs, and the results are presented in Fig. 11. It is obvious from the figure that there is a good correlation between q_e and the solution temperate (R^2 was 0.9769 for MWCNTs 10–20 and 0.9971 for MWCNTs 40–60). These results indicate that the adsorption of aniline from an aqueous solution by MWCNTs obeys a pseudo-second order kinetic model.

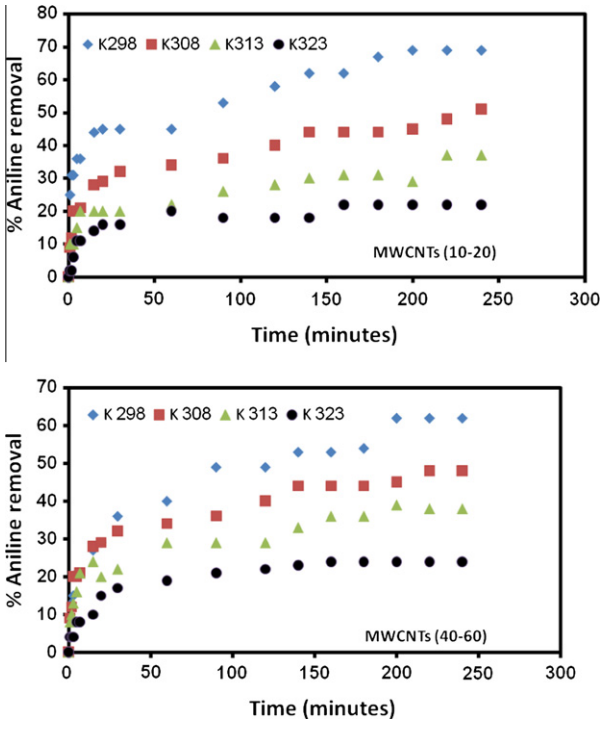

Fig. 9. Effect of solution temperature on the kinetics of aniline adsorption from an aqueous solution by different MWCNTs. (experimental conditions: 20 ml solution, pH 7.0, 30 mg CNTs, and aniline concentration 50 mg/l).

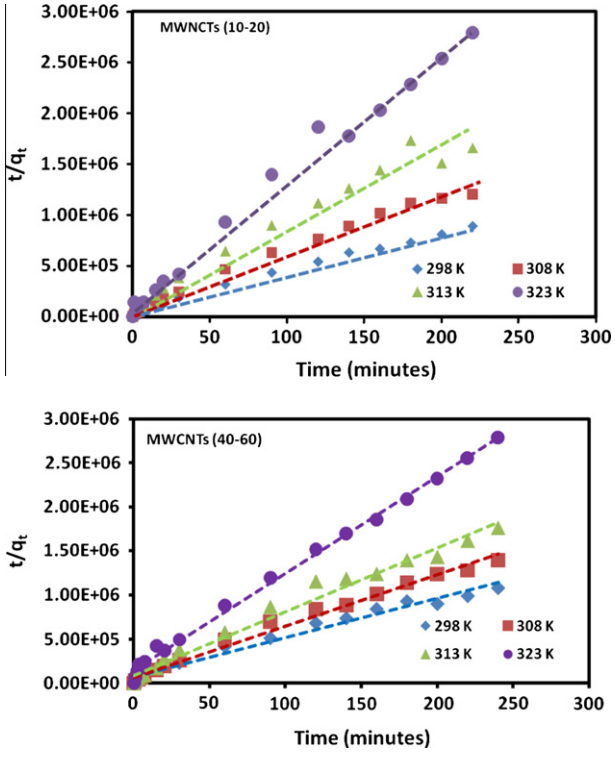

Fig. 10. Plots of the pseudo-second order kinetics of aniline adsorption on pristine MWCNTs (linear form). (experimental conditions: 20 ml solution, pH 7.0, 30 mg CNTs, and aniline concentration 50 mg/l).

Table 2
Parameters of the pseudo-second-order kinetic models for the adsorption of aniline on pristine MWCNTs.

Temperature (K)	MWCNTs (10–20 nm)			MWCNTs (40–60 nm)		
	k_2	q_e ($\times 10^{-4}$)	R^2	k_2	q_e ($\times 10^{-4}$)	R^2
298	533.43	2.49	0.9859	276.08	2.24	0.9824
308	729.24	1.74	0.994	540.38	1.71	0.9902
313	832.54	1.24	0.9771	600.42	1.38	0.9836
323	1732.218	0.799	0.9908	845.36	0.907	0.9962

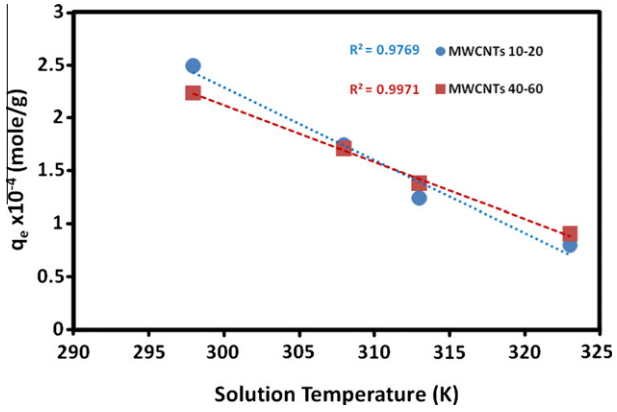

Fig. 11. The relationship between the calculated amounts of aniline adsorbed on MWCNTs at equilibrium (q_e) and the solution temperature. (experimental conditions: 20 ml solution, pH 7.0, 30 mg CNTs, and aniline concentration 50 mg/l).

A similar phenomenon was observed for the adsorption of aniline on Cr-bentonite [42] and activated carbon [43].

As previously stated, the adsorption of aniline on MWCNTs occurred in two steps. The faster first step could be attributed to the diffusion of the aniline molecules from the aqueous phase to the outer-surface of the solid MWCNTs. The slower second step could be attributed to the intra-particle diffusion of the aniline molecules between the MWCNTs aggregates. The probability of intra-particle diffusion was explored by using the intra-particle diffusion model [44]:

$$q_t = k_{id} t^{1/2} + C \tag{4}$$

where q_t is adsorption capacity at any time (t), k_{id} is the intra-particle diffusion rate constant (mole/g min$^{1/2}$) and C (mole/g) is a constant proportional to the thickness of the boundary layer. Plotting q_t versus $t^{1/2}$, "Weber–Morris plot" [44], provides an indication of the dependency of adsorption on intra-particle diffusion. If the plot produces a straight line, then the adsorption process is controlled by intra-particle diffusion only. If it exhibits multi-linear plots, then there are two or more steps affecting the adsorption process. Fig. 12 shows the Weber–Morris plot of the aniline adsorption by MWCNTs. It is clear from the figure that the removal of aniline by both MWCNTs occurred in two different steps as the plot contains two different straight lines. The first line from 0 to 20 min was attributed to the fast diffusion of the aniline molecules from the aqueous phase to the MWCNTs surface. The second line from 20 min to 220 min was due to the intra-particle diffusion. The amount of aniline adsorbed (q_t) was found to be linearly correlated with $t^{1/2}$ at different temperatures. The correlation coefficients (R^2) were greater than 0.94, indicating that the adsorption mechanism followed the intra-particle diffusion process. This confirms that the adsorption of aniline by MWCNTs was a multi-step process and involved the adsorption to the external surface and diffusion. The mechanism of the removal of aniline by adsorption is assumed

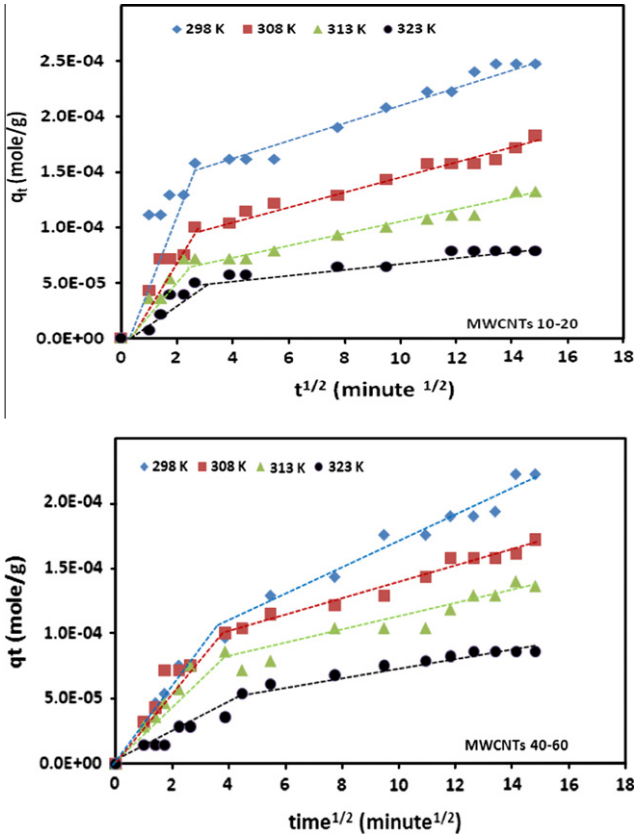

Fig. 12. Intra-particle diffusion plots of aniline on MWCNTs at different temperatures. (experimental conditions: 20 ml solution, pH 7.0, 30 mg CNTs, and aniline concentration 50 mg/l).

to involve the following steps: (1) migration of aniline from the bulk solution to the external surface of MWCNTs; (2) diffusion of aniline through the boundary layer to the external surface of MWCNTs; (3) adsorption of aniline at an active site on the surface of ash; (4) intra-particle diffusion and adsorption of aniline through the MWCNTs particles. Table 3 presents the values for the intra-particle diffusion parameters obtained from the slope and intercept of the graph in Fig. 12. The intra-particle diffusion rate constant, k_{id}, was in the range of 4.0–10 $\times 10^{-6}$ (mol/g min$^{1/2}$) for both MWCNTs. As presented in Fig. 13, the intra-particle diffusion rate constant (k_{id}) was found to be linearly correlated with $t^{1/2}$ at different temperatures and revealed the dependency of intra-particle diffusion of aniline on the solution temperature. The driving force of diffusion is very important in adsorption processes. While the intra-particle diffusion model has indicated that aniline adsorption by MWCNTs is the rate-determining step, it does not sufficiently indicate which of the two steps (surface adsorption or intra-particle diffusion) was the limiting step. As it is essential for the q_t versus $t^{1/2}$ plots to go though the origin if intra-particle diffusion is the sole rate limiting step [45], and because the values of C range from 4.0 $\times 10^{-6}$ to 10 $\times 10^{-6}$ (mol/g min$^{1/2}$), it may be concluded that the surface adsorption and intra-particle diffusion occurred concurrently during the adsorption of aniline by MWCNTs.

The pseudo-second order rate constant for the removal of aniline could be expressed as a function of temperature by the Arrhenius type relationship, as shown in following equation:

$$\ln k_2 = \ln A - \frac{E_a}{RT} \tag{5}$$

where E_a is the Arrhenius activation energy of adsorption, representing the minimum energy that reactants must have for the

Table 3
Intra-particle diffusion parameters for the adsorption of aniline from an aqueous solution by different MWCNTs at different temperatures.

Temperature (K)	MWCNTs (10–20 nm)			MWCNTs (40–60 nm)		
	k_{id} (mol/g min$^{1/2}$)	C (mol/g)	R^2	k_{id} (mol/g min$^{1/2}$)	C (mol/g)	R^2
298	9.0×10^{-6}	10.0×10^{-5}	0.976	10.0×10^{-6}	6.0×10^{-5}	0.967
308	6.0×10^{-6}	8.0×10^{-5}	0.977	6.0×10^{-6}	8.0×10^{-5}	0.975
313	5.0×10^{-6}	5.0×10^{-5}	0.969	6.0×10^{-6}	5.0×10^{-5}	0.946
323	2.0×10^{-6}	5.0×10^{-5}	0.946	3.0×10^{-6}	4.0×10^{-5}	0.959

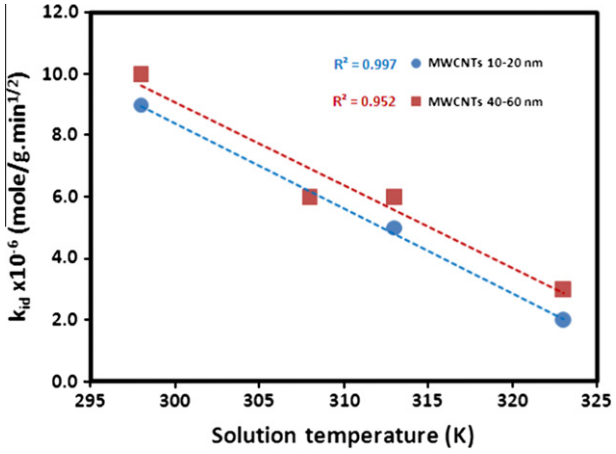

Fig. 13. The relationship between the calculated intra-particle diffusion rate constant (K_{id}) and the solution temperature for the adsorption of aniline by different MWCNTs. (experimental conditions: 20 ml solution, pH 7.0, 30 mg CNTs, and aniline concentration 50 mg/l).

reaction to proceed, A is the Arrhenius factor, R the gas constant and is equal to 8.314 J mol^{-1} K^{-1}, and T is the solution temperature.

As shown in Fig. 14, the slopes of the linear plots of ln k_2 versus $1/T$ for the adsorption of aniline by MWCNTs 10–20 and MWCNTs 40–60 were constructed to calculate the adsorption activation energy. The adsorption activation energies obtained were 36.79 and 35.27 kJ mol^{-1} for MWCNTs 10–20 and MWCNTs 40–60, respectively. Low activation energies are characteristic of a physical adsorption (5–40 kJ mol^{-1}), while higher activation energies (40–800 kJ mol^{-1}) suggest chemical adsorption [46]. The chemical (chemisorption) or physical adsorption (physisorption) mechanisms are often an important indicator to describe the type of interaction between the organic pollutants, such aniline molecules, and adsorbents, such as MWCNTs. The pseudo-second order

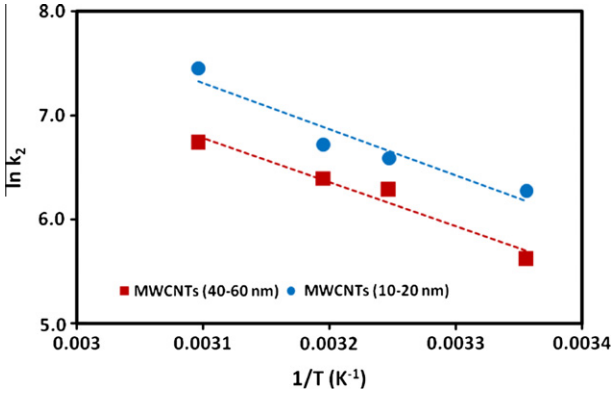

Fig. 14. Arrhenius plot of the pseudo-second order kinetics for the adsorption of aniline on different MWCNTs. (experimental conditions: 20 ml solution, pH 7.0, 30 mg CNTs, and aniline concentration 50 mg/l).

adsorption capacity (q_e) for aniline by MWCNTs (from Fig. 11), which decreases with increasing temperature, was determined to be a physisorption process.

Thermodynamic parameters were evaluated to confirm the nature of the adsorption of the aniline by MWCNTs. The thermodynamic parameters including the Gibbs free energy change (ΔG°), enthalpy change (ΔH°) and entropy change (ΔS°) were calculated to evaluate the thermodynamic feasibility and spontaneous nature of the process. These parameters were calculated from the variation of the thermodynamic equilibrium constant K_0 with respect to temperature [22,47]. K_0 for the adsorption reaction can be defined as follows:

$$K_0 = \frac{a_s}{a_e} = \frac{\gamma_s (C_s/C_s^0)}{\gamma_e (C_e/C_e^0)} \tag{6}$$

where a_s and a_e are the activities of adsorbed aniline on the MWCNTs surface and in solution at equilibrium, respectively, C_s is the surface concentration of aniline in mole per gram of MWCNTs, C_e is the aqueous concentration of aniline at equilibrium (mole/l), C_s^0 is the surface concentration of aniline at a monolayer coverage of the adsorbent, C_e^0 is molar concentration of aniline at standard conditions and is equal to 1 M, γ_s is the activity coefficient of the adsorbed aniline and γ_e is the activity coefficient of the aniline in solution. In dilute solutions and at low surface coverage the activity coefficients approach unity, reducing Eq. (6) to the following form:

$$K_0 = \frac{C_s/C_s^0}{C_e/C_e^0} \tag{7}$$

The standard free energy change (ΔG°) for adsorption was calculated from the following relationship:

$$\Delta G^\circ = -RT \ln(K_0) \tag{8}$$

where R is the universal gas constant, and T is the temperature in Kelvin. Using the Van't Hoff equation, the average standard enthalpy change (ΔH°) can be calculated from the relationship between K_0 and T:

$$\ln(K_0) = \frac{-\Delta H^\circ}{RT} + \text{const} \tag{9}$$

and standard entropy changes (ΔS°) can be calculated from:

$$\Delta G^\circ = \Delta H^\circ - T\Delta S^\circ \tag{10}$$

Using the above relationships, the thermodynamic parameters, including the standard free energy change (ΔG°), the standard enthalpy change (ΔH°), and the change in the entropy (ΔS°), were calculated from the variation of the thermodynamic equilibrium constant K_0 with respect to temperature. Table 4 summarizes the variations of the thermodynamic parameters for the adsorption of aniline on the MWCNTs 10–20 and MWCNTs 40–60.

In general, the adsorption equilibrium constant, K_0, increased by decreasing the temperature for both MWCNTs. The following K_0 values were calculated at 298 K, 308 K, 313 K, and 323 K, respectively: 5.41, 5.01, 4.77, 4.48 for MWCNTs 10–20; and 5.20, 4.90, 4.71, and 4.47 for MWCNTs 40–60. The standard free energy change, ΔG°, is negative for both MWCNTs. The negative value of

Table 4
Values of the different thermodynamic parameters for the adsorption of aniline on different MWCNTs.

Temperature (K)	ln K_o	$\Delta G°$ (kJ/mol)	$\Delta H°$ (kJ/mol)	$\Delta S°$ (J/K mol)
MWCNTs (10–20 nm)				
298	5.41	−12.28	−30.11	−65.33
308	5.01	−11.37	−30.11	−68.67
313	4.77	−10.84	−30.11	−70.62
323	4.48	−10.167	−30.11	−73.07
MWCNTs (40–60 nm)				
298	5.20	−12.89	−23.94	−37.06
308	4.90	−12.56	−23.94	−36.94
313	4.71	−12.26	−23.94	−37.32
323	4.47	−11.99	−23.94	−36.98

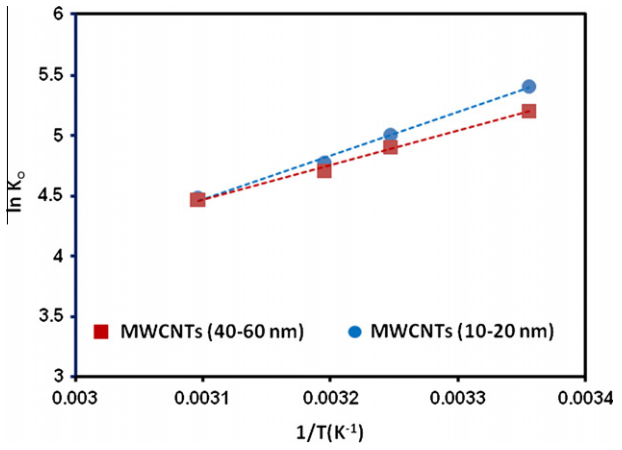

Fig. 15. Plot of ln K_C versus $1/T$ to estimate the thermodynamic parameters for the adsorption of aniline on different MWCNTs. (experimental conditions: 20 ml solution, pH 7.0, 30 mg CNTs, and aniline concentration 50 mg/l).

$\Delta G°$ was expected for a product favored reaction. These values became more negative as the temperature increased, indicating the exothermic nature of the adsorption of aniline by MWCNTs. Fig. 15 shows the Van't Hoff plot for the adsorption of aniline on both MWCNTs. It is clear from Fig. 15 and Table 4 that the negative values of $\Delta H°$ verify the exothermic nature of aniline adsorption on different MWCNTs. This observation explains the decrease in adsorption at lower temperature. The negative values of $\Delta S°$ suggested the decrease in randomness at the solid/solution interface during the adsorption of aniline on MWCNTs. The negative entropy of the adsorption and immobilization of aniline on the MWCNTs surface may be attributed to the decrease in the degree of freedom of aniline molecules.

4. Conclusions

The removal of aniline from an aqueous solution by pristine multi-walled carbon nanotubes was studied. The effect of varying parameters that affect the removal/adsorption process such as aniline concentration, carbon nanotubes mass, solution temperature, and pH were investigated using two multi-walled carbon nanotubes. The adsorption of aniline on pristine MWCNTs at different temperatures was studied kinetically and thermodynamically. The kinetic study revealed that the adsorption follows a pseudo-second order process and occurred in two steps. The first step was the diffusion of the aniline from the aqueous solution to the outer surface of the multi-walled carbon nanotubes. The second slower step involved aniline molecules diffusion through the nanotubes. The thermodynamic study revealed that the adsorption process is product favored and becomes less so by increasing the temperature because the adsorption is exothermic. The change in entropy values was negative which indicated a decrease in randomness due to the transfer of aniline molecules from the aqueous phase to the surface of the carbon nanotubes. We have shown that carbon nanotubes can be considered a potential and promising adsorbent for the removal of aniline, a typical organic pollutant, from an aqueous solution.

References

[1] W. Chu, W.K. Choy, T.Y. So, J. Hazard. Mater. 141 (2007) 86–91.
[2] C. Karunakaran, S. Senthilvelan, Sol. Energy 79 (2005) 505–512.
[3] A. Kumar, N. Mathur, J. Colloid Interface Sci. 300 (2006) 244–252.
[4] Y. Han, X. Quan, S. Chen, H. Zhao, C. Cui, Y. Zhao, Sep. Purif. Technol. 50 (2006) 365–372.
[5] F. Villacanas, M.F.R. Pereira, J.J.M. Órfão, J.L. Figueiredo, J. Colloid Interface Sci. 293 (2006) 128–136.
[6] K. László, Colloid Surf., A 265 (2005) 32–39.
[7] N. Jagtap, V. Ramaswamy, Appl. Clay Sci. 33 (2006) 89–98.
[8] H.T. Gomes, P. Selvam, S.E. Dapurkar, J.L. Figueiredo, J.L. Faria, Microporous Mesoporous Mater. 86 (2005) 287–294.
[9] L. Wang, S. Barrington, J. Kim, J. Environ. Manage. 83 (2007) 191–197.
[10] W.M. Zhang, Q.J. Zhang, B.C. Pan, L. Lv, B.J. Pan, Z.W. Xu, Q.X. Zhang, X.S. Zhao, W. Du, Q.R. Zhang, J. Colloid Interface Sci. 306 (2006) 216–221.
[11] K. Yang, W. Wu, Q. Jing, L. Zhu, Environ. Sci. Technol. 42 (2008) 7931–7936.
[12] X. Li, H. Zhao, X. Quan, S. Chen, Y. Zhang, H. Yu, J. Hazard. Mater. 186 (2011) 407–415.
[13] G. Sheng, D. Shao, X. Ren, X. Wang, J. Li, Y. Chen, X. Wang, J. Hazard. Mater. 178 (2010) 505–516.
[14] Q. Zhou, J. Xiao, W. Wang, J. Chromatogr. A 1125 (2006) 152–158.
[15] C. Basheer, A.A. Alnedhary, B.S.M. Rao, S. Valiyaveettil, H.K. Lee, Anal. Chem. 78 (2006) 2853–2858.
[16] Q. Zhou, W. Wang, J. Xiao, Anal. Chem. Acta 559 (2006) 200–206.
[17] G. Min, S. Wang, H. Zhu, G. Fang, Y. Zhang, Sci. Total Environ. 396 (2008) 79–85.
[18] X.M. Yan, B.Y. Shi, J.J. Lu, C.H. Feng, D.S. Wang, H.X. Tang, J. Colloid Interface Sci. 321 (2008) 30–38.
[19] Q. Zhou, W. Wang, J. Xiao, J. Wang, G. Liu, Q. Shi, G. Guo, Microchim. Acta 152 (2006) 215–224.
[20] M. Abdel Salam, M. Mokhtar, S.N. Basahel, S.A. Al-Thabaiti, A.Y. Obaid, J. Alloys Compd. 500 (2010) 87–92.
[21] M. Abdel Salam, R. Burk, Water, Air, Soil Pollut. 210 (2010) 101–111.
[22] M. Abdel Salam, R. Burk, Appl. Surf. Sci. 255 (2008) 1975–1981.
[23] M. Abdel Salam, R. Burk, J. Sep. Sci. 32 (2009) 1060–1068.
[24] M. Abdel Salam, R. Burk, Anal. Bioanal. Chem. 390 (2008) 2159–2170.
[25] I. Fasfous, E. Radwan, J. Dawoud, Appl. Surf. Sci. 256 (2010) 7246–7252.
[26] A. Ambrosi, R. Antiochia, L. Campanella, R. Dragone, I. Lavagnini, J. Hazard. Mater. 122 (2005) 219–225.
[27] C. Pan, S. Xu, H. Zou, Z. Guo, Y. Zhang, B. Guo, J. Am. Soc. Mass Spectrom. 16 (2005) 263–270.
[28] A.S. Brady-Estévez, T.H. Nguyen, L. Gutierrez, M. Elimelech, Water Res. 44 (2010) 3773–3780.
[29] P. Kueseng, C. Thammakhet, P. Thavarungkul, P. Kanatharana, Microchem. J. 96 (2010) 317–323.
[30] Q. Zhou, Y. Ding, J. Xiao, Anal. Bioanal. Chem. 385 (2006) 1520–1525.
[31] W.D. Wang, Y.M. Huang, W.Q. Shu, J. Cao, J. Chromatogr. A 1173 (2007) 27–30.
[32] S. Wang, P. Zhao, G. Min, G. Fang, J. Chromatogr. A 1165 (2007) 166–171.
[33] P. Liang, Q. Ding, F. Song, J. Sep. Sci. 28 (2005) 2339–2343.
[34] P. Liang, Y. Liu, L. Guo, J. Zeng, H. Lu, J. Anal. At. Spectrom. 19 (2004) 1489–1492.
[35] A. Stafiej, K. Pyrzynska, Sep. Purif. Technol. 58 (1) (2007) 49–52.
[36] G.P. Rao, C. Lu, F. Su, Sep. Purif. Technol. 58 (2007) 224–231.
[37] M. Tuzen, K.O. Saygi, M. Soylak, J. Hazard. Mater. 152 (2008) 632–639.
[38] Z. Gaoa, T. Bandoszc, Z. Zhao, M. Hand, J. Qiu, J. Hazard. Mater. 167 (2009) 357–365.
[39] X. Xie, L. Gao, J. Sun, Colloids Surf., A 308 (2007) 54–59.
[40] Y.F. Sun, A.M. Zhang, Y. Yin, Y.M. Dong, Y.C. Cui, X. Zhang, J.M. Hong, Mater. Chem. Phys. 101 (2007) 30–34.
[41] K. László, E. Tombácz, C. Novák, Colloids Surf., A 306 (2007) 95–101.
[42] H. Zheng, D. Liu, Y. Zheng, S. Liang, Z. Liu, J. Hazard. Mater. 167 (2009) 141–147.
[43] C. Valderrama, J.I. Barios, M. Caetano, A. Farran, J.L. Cortina, React. Funct. Polym. 70 (2010) 142–150.
[44] W.J. Weber Jr., J.C. Morris, Sanit. Eng. Div. ASCE 89 (SA2) (1963) 31–59.
[45] Y.S. Ho, Water Res. 37 (10) (2003) 2323–2330.
[46] H. Nollet, M. Roels, P. Lutgen, P. Van der Meeren, W. Verstraete, Chemosphere 53 (2003) 655–665.
[47] A. Dąbrowski, P. Podkościenly, Z. Hubicki, M. Barczak, Chemosphere 58 (2005) 1049–1070.